Proceedings of the Fifteenth International Conference on
Computational Structures Technology
Edited by: P. Iványi, J. Kruis and B.H.V. Topping
Civil-Comp Conferences, Volume 9, Paper 3.4
Civil-Comp Press, Edinburgh, United Kingdom, 2024
ISSN: 2753-3239, doi: 10.4203/ccc.9.3.4

Uniform Multiple Laminates Interpolation Method for Angle Optimization of Double-Double Composite Laminates Based on Multi-Material Topology Optimization Strategy

P. Fang[1], T. Gao[1], Y. Huang[1], P. Duysinx[2], W. Zhang[1] and L. Song[1]

[1]School of Mechanical Engineering, Northwestern Polytechnical University, Xi'an, China
[2]Department of Aerospace and Mechanical Engineering, University of Liège, Liège, Belgium

Abstract

Double-Double laminates present an innovative laminate layup, incorporating a repetition of sub-plies featuring two groups of balanced angles. This layup provides composite materials a broad design flexibility together with the ease of design and manufacturing. This paper proposes an optimization design method for Double-Double laminates based on multi-material topology optimization, which can be applied to the angle optimization design of composite structures with Double-Double layups. A uniform multiple laminates interpolation model is proposed to describe the certainty of the layer direction of composite laminates. The uniform multiple laminates interpolation has the additional advantage when dealing with multi-area and multi-layer composite structures, as it significantly reduces the number of calculations required and eliminates the need for adding interlayer constraints during optimization. The stiffness matrix of each combination of angles for Double-Double laminates is interpolated to form virtual laminates. The sensitivity of the optimization problem with the objective of minimizing the compliance is derived. Finally, the method was applied to the design of composite stiffened panels and composite Unmanned Aerial Vehicle wing. The optimal results show that the optimized Double-Double laminates can get better performance than the Quad laminates with the same percentage of angle.

Keywords: composite structures, Double-Double laminates, multi-material topology optimization, discrete material, uniform multiple laminates interpolation, ply orientation angle design.

1 Introduction

Composite materials are typically manufactured as fiber-reinforced laminate structures, widely used in aerospace and other high-performance applications due to their exceptional specific strength and stiffness[1], [2]. The properties of composite laminates, including stiffness, strength, and buckling behavior, are closely linked to the fiber orientation and lamination thickness. As such, optimizing the fiber angle design has become a highly sought-after objective in the structural design of composite laminates to achieve superior performance.

The alternative angles of composite laminates are typically discrete rather than continuous. Consequently, the angle optimization problem of composite structures can reformulated as a multi-material topology optimization problem where each alternative angle is regarded as an independent material. The uniform multiphase materials interpolation (UMMI) scheme[3] which is known as discrete material optimization (DMO) and firstly proposed by Stegmann and Lund[4], is a typical method. The UMMI approach can converge to one of the alternative angles for each element by penalizing the intermediate elemental angles which are interpolated from the alternative angles with equal weights ranging from 0 to 1. The results demonstrate that this method can be applied to stiffness optimization design[5], natural frequency optimization design[6], and local dynamic response of composite materials[7]. However, optimization design of composite ply angles in practical engineering remains a challenging task due to the constraints imposed by the manufacturing process[8-12].

Double-double (DD) laminates proposed by Tsai[13] provide a fresh and innovative solution by incorporating a repetition of sub-plies featuring two groups of balanced angles. Due to its special stacking sequence, DD laminates yield more homogenized bending properties compared to the conventional Quad laminates, which only includes 0, ±45, and 90 degree angles. Simultaneously, DD laminate meet most of the above-mentioned design constraints in stacking direction, while keeping the simplicity of a four plies of sub-plies. Moreover, DD laminates can provide a lightweight design for easy tapering. All these advantages of DD laminates attract the attention of many researchers from both academic and industry.

Shrivastava et al[14]. used artificial intelligence genetic algorithm to optimize the wing quality of DD laminates by considering unit-circle failure, buckling mode and wing-tip deflection design criteria. Zhao[15] et al. proposed a new formula for calculating the lamination parameters of DD laminates. On this basis, the feasible region of any combination of two lamination parameters is obtained by using Lagrange multiplier analysis. Vermes[16] et al. proposed the lamination method and advantages of DD laminates. The DD lamination method can significantly reduce the number of plies required for laminates, thereby reducing the weight of the composite structure. Kappel[17] et al. proposed an optimization method based on failure envelope circle to optimize the design of DD laminates. Wang[18] et al. proposed a nested p-norm method integrating the Tsai–Hill failure criterion indexes of different elements in different plies into one design response, thus realizing the effective stress

control for topology optimization of laminated structures. Tsai' lam[19] search approach can identify the best DD angles by listing the possible angles with a specified angle interval. However, to the authors' knowledge, there are few researches on the angle design of DD laminates.

2 Methods

DD laminates are multi-layer structures as shown in Figure 1, such as [+Φ/-Ψ/-Φ/+Ψ]NT, where N represents the number of repetitions of the sub-plies and T denotes the total number of plies. This means that once the stacking sequence of the sub-plies and total thickness of the DD laminate are determined, the stacking sequence of the DD laminate is also determined. Optimizing DD laminates using UMMI scheme cannot describe the certainty of the stacking direction of DD laminates. In addition, DD laminates naturally meet most existing design constraints because the stacking direction is formed by repeated sub-plies. So, the optimal design of DD laminates is different from optimizing the fiber angle selection in single-layer laminates or the stacking sequence in multi-layer structures.

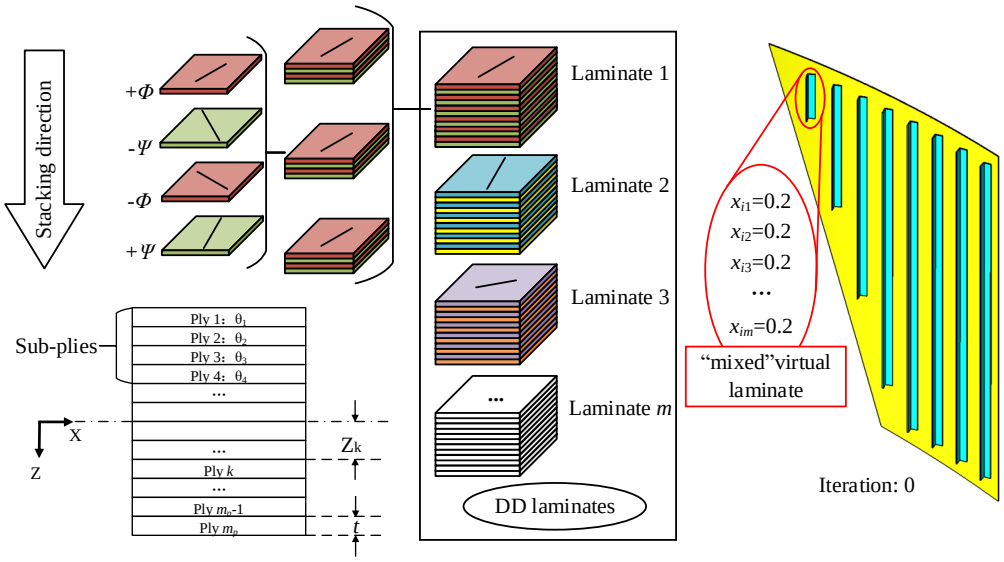

Figure 1 The application of UMLI to the DD laminates

Therefore, in order to describe the fixed stacking sequence of the plies in DD laminates, we consider the combination of many plies as a whole, rather than as many separate plies. The uniform multiple laminates interpolation (UMLI) scheme inspired by UMMI, which interpolates the stiffness matrix of the laminate is proposed. As shown in Figure 1, if each area has m_L alternative DD laminates, the $\boldsymbol{A}$ $\boldsymbol{B}$ $\boldsymbol{D}$ matrix of the ith element is represented as a virtual laminate formed by the weighted sum of alternating angle combinations.

$$\begin{bmatrix} \boldsymbol{A} & \boldsymbol{B} \\ \boldsymbol{B} & \boldsymbol{D} \end{bmatrix}_i = \sum_{j=1}^{m_L} w_{ij} \begin{bmatrix} \boldsymbol{A} & \boldsymbol{B} \\ \boldsymbol{B} & \boldsymbol{D} \end{bmatrix}_i^{(j)} \tag{1}$$

Herein A is the tensile stiffness matrix of the laminates, B is the coupling stiffness matrix, and D is the bending stiffness matrix. The relationship between design variables xij and weighting function wij in UMMI is as follows, and each individual element encompasses mL design variables.

$$w_{ij} = x_{ij}^{p} \prod_{\substack{\xi=1 \\ \xi \neq j}}^{m_L} \left(1 - x_{i\xi}^{p}\right) \tag{2}$$

To have a clear idea, the number of design variables for each individual element needed for UMLI and UMMI schemes is shown in Figure 2. When the angle increment Δ is 7.5 degrees, the design variables of the each individual element of UMLI are always 91 (the number of alternative laminates). The design variables of the each individual element of UMMI increase with the number of plies, and are 720 at 30 plies.

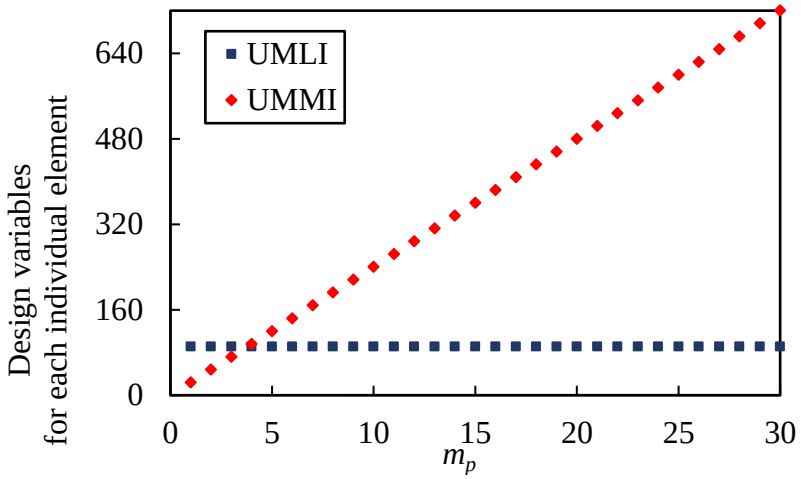

Figure 2 Comparison of the number of design variables for each individual element related to UMLI and UMMI.

The derivation of the A B D matrix for DD laminates is presented below. The relationship between internal moment and strain can be expressed as:

$$\begin{aligned} \boldsymbol{P} &= \begin{bmatrix} \boldsymbol{P}_x \\ \boldsymbol{P}_y \\ \boldsymbol{P}_{xy} \end{bmatrix} = \sum_{k=1}^{m_p} \int_{z_{k-1}}^{z_k} \overline{\boldsymbol{Q}}\, \mathrm{d}z\boldsymbol{\varepsilon}^0 + \sum_{k=1}^{m_p} \int_{z_{k-1}}^{z_k} \overline{\boldsymbol{Q}}\, z\mathrm{d}z\boldsymbol{\kappa} = \boldsymbol{A}\boldsymbol{\varepsilon}^0 + \boldsymbol{B}\boldsymbol{\kappa} \\ \boldsymbol{M} &= \begin{bmatrix} \boldsymbol{M}_x \\ \boldsymbol{M}_y \\ \boldsymbol{M}_{xy} \end{bmatrix} = \sum_{k=1}^{m_p} \int_{z_{k-1}}^{z_k} \overline{\boldsymbol{Q}}\, z\mathrm{d}z\boldsymbol{\varepsilon}^0 + \sum_{k=1}^{m_p} \int_{z_{k-1}}^{z_k} \overline{\boldsymbol{Q}}\, z^2\mathrm{d}z\boldsymbol{\kappa} = \boldsymbol{B}\boldsymbol{\varepsilon}^0 + \boldsymbol{D}\boldsymbol{\kappa} \end{aligned} \tag{3}$$

Herein $\boldsymbol{P}$ and $\boldsymbol{M}$ are vectors of the in-plane forces and moments per unit width. m_p is the total number of plies of the laminates. z_k, $z_{k-1}$is the coordinates of the upper and lower surfaces of ply $\boldsymbol{k}$. $\boldsymbol{\varepsilon}^0$ is the middle plane strain vector, $\boldsymbol{\kappa}$ is the middle plane curvature vector. The calculated $\boldsymbol{A}$ $\boldsymbol{B}$ $\boldsymbol{D}$ matrix can be expressed as:

$$\boldsymbol{A}=\sum_{k=1}^{n}\overline{\boldsymbol{Q}_k}\left(z_k-z_{k-1}\right);\ \boldsymbol{B}=\sum_{k=1}^{n}\overline{\boldsymbol{Q}_k}\left(\frac{z_k{}^2-z_{k-1}{}^2}{2}\right);\ \boldsymbol{D}=\sum_{k=1}^{n}\overline{\boldsymbol{Q}_k}\left(\frac{z_k{}^3-z_{k-1}{}^3}{3}\right) \tag{4}$$

As DD laminates are composed of two angles in a certain stacking sequence to form four-ply sub-plies, and then the repeatedly formed laminates are shown in Figure 1, so the stiffness matrix $\boldsymbol{A}$ $\boldsymbol{B}$ $\boldsymbol{D}$ of DD laminates can be simplified as follows:

$$\begin{aligned}\boldsymbol{A}&=Nt\left(\overline{\boldsymbol{Q}_1}+\overline{\boldsymbol{Q}_2}+\overline{\boldsymbol{Q}_3}+\overline{\boldsymbol{Q}_4}\right);\boldsymbol{B}=\frac{3Nt^2}{2}\left(\overline{\boldsymbol{Q}_4}-\overline{\boldsymbol{Q}_1}\right)+\frac{Nt^2}{2}\left(\overline{\boldsymbol{Q}_3}-\overline{\boldsymbol{Q}_2}\right)\\ \boldsymbol{D}&=\left(\frac{4N^3}{3}+N\right)t^3\left(\overline{\boldsymbol{Q}_1}+\overline{\boldsymbol{Q}_4}\right)+\left(\frac{4N^3}{3}-N\right)t^3\left(\overline{\boldsymbol{Q}_2}+\overline{\boldsymbol{Q}_3}\right)\end{aligned} \tag{5}$$

Herein, N is the number of sub-plies, $N= m_p/4$. t is the thickness of the ply. $\overline{\boldsymbol{Q}_1}$ $\overline{\boldsymbol{Q}_2}$ $\overline{\boldsymbol{Q}_3}$ $\overline{\boldsymbol{Q}_4}$ are the unidirectional plate off-axis stiffness matrices that form the sub-plies of 4 plies, and if the stacking sequence of the sub-plies is [+Φ/-Ψ/-Φ/+Ψ], then $\overline{\boldsymbol{Q}_1}=\overline{\boldsymbol{Q}_{\Phi}}$, $\overline{\boldsymbol{Q}_2}=\overline{\boldsymbol{Q}_{-\Psi}}$, $\overline{\boldsymbol{Q}_3}=\overline{\boldsymbol{Q}_{-\Phi}}$, $\overline{\boldsymbol{Q}_4}=\overline{\boldsymbol{Q}_{\Psi}}$.

The alternative angle range for conventional laminates is -90 to 90 degrees. The relationship between the number of alternative angles m and the angle increment is shown in Equation(6). When the angle increment Δ is 7.5 degrees, there are 24 possibilities [0, 7.5, 15, …, 82.5, 90, -82.5, …, -15, -7.5]. The usual angle increment is taken as 45 degrees, and the angle selection for laminate is [0, 45, 90, -45], which is called Quad.

$$m_v=\frac{180^\circ}{\Delta} \tag{6}$$

While the value range of the alternative angle combinations [Φ/Ψ] for DD laminates is 0 to 90 degrees. The relationship between the number of alternative angles m_L and the angle increment is shown in Equation(7). If the angle increment is 7.5 degrees, then there are 13 choices for each of Φ and Ψ. After permutation and combination, the number of possible angle combinations for DD laminates is 91 as shown in Figure 3. The horizontal axis represents the value of Φ, while the vertical axis represents the value of Ψ. The squares indicate the angle combination numbers.

$$m_L=\frac{\left(\frac{90^\circ}{\Delta}+2\right)\left(\frac{90^\circ}{\Delta}+1\right)}{2} \tag{7}$$

The so-called single-double (SD) laminates should be highlight. SD means $\Phi=\Psi$ (blue in Figure 3) and is a better choice in some applications, because compared to DD, SD has more fibers which can achieve a smaller angle with the principal stress. Among SD, there is special case. Plus or minus 0 degrees results is the same angle, as well as plus or minus 90 degrees. If $\Phi=\Psi$ is equal to 0 or 90 degrees (red in Figure 3**Hiba! A hivatkozási forrás nem található.**), it means that each ply of the laminates has the same angle. While this is typically not allowed in engineering due to manufacturability constraints, the mechanical properties of this stacking sequence are strongest in the 0 or 90 degree orientation. In the subsequent example, we will analyze the impact of excluding laminates with the same angle plying and laminates with SD stacking sequences from the alternative angle combination on the optimization results.

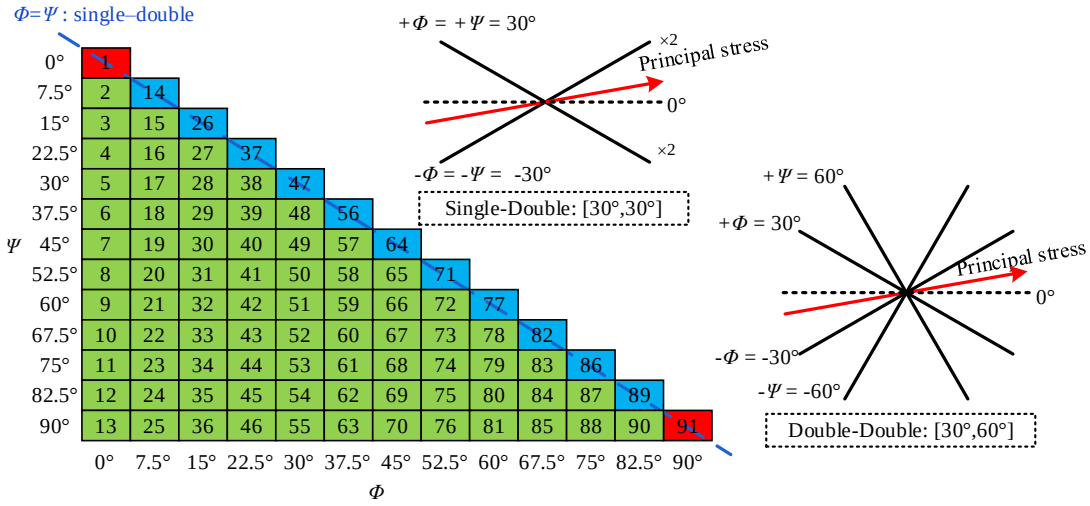

Figure 3 [Φ/Ψ] Angle combinations with an angle increment of 7.5.

Considering the minimum compliance of composite laminates. Optimization problems can be described as:

$$\begin{aligned} &\text{find}: \left\{x_{ij}\right\} \quad \left(i=1,\cdots,m_e; j=1,\cdots,m_L\right) \\ &\text{minimize}: \ C=\boldsymbol{F}^{\mathrm{T}}\boldsymbol{u} \\ &\text{subject to}: \ \boldsymbol{F}=\boldsymbol{K}\boldsymbol{u} \end{aligned} \tag{8}$$

Herein x_{ij} is the design variable. m_e is the number of elements and m_L is the number of angle combinations for DD laminates. C is the overall compliance. $\boldsymbol{K}$ is the element stiffness matrix. $\boldsymbol{F}$ and $\boldsymbol{u}$ are the external force vector and the displacement vector, respectively.

The sensitivity of the overall compliance can be generally expressed as:

$$\frac{\partial C}{\partial x_{ij}}=2\boldsymbol{u}^{\mathrm{T}}\frac{\partial \boldsymbol{F}}{\partial x_{ij}}-\boldsymbol{u}^{\mathrm{T}}\frac{\partial \boldsymbol{K}}{\partial x_{ij}}\boldsymbol{u} \tag{9}$$

For fixed loads, then we have $\frac{\partial \boldsymbol{F}}{\partial x_{ik}} \equiv 0$. Thus, the sensitivity can be simplified as

$$\frac{\partial C}{\partial x_{ij}} = -\boldsymbol{u}^{\mathrm{T}} \frac{\partial \boldsymbol{K}}{\partial x_{ij}} \boldsymbol{u} = -\boldsymbol{u}_i^{\mathrm{T}} \frac{\partial \boldsymbol{K}_i}{\partial x_{ij}} \boldsymbol{u}_i \tag{10}$$

Here, the stiffness matrix of element *i* is defined as:

$$\boldsymbol{K}_i = \iint \begin{bmatrix} \boldsymbol{B}_p \\ \boldsymbol{B}_b \end{bmatrix}_i^{\mathrm{T}} \begin{bmatrix} \boldsymbol{A} & \boldsymbol{B} \\ \boldsymbol{B} & \boldsymbol{D} \end{bmatrix}_i \begin{bmatrix} \boldsymbol{B}_p \\ \boldsymbol{B}_b \end{bmatrix}_i dxdy \tag{11}$$

Where $\left[\boldsymbol{B}_p\right]$ and $\left[\boldsymbol{B}_b\right]$ are relations between strain and displacement vectors.

$$\left\{\boldsymbol{\kappa}\right\} = \left[\boldsymbol{B}_b\right]\left\{\boldsymbol{u}_b\right\};\ \left\{\boldsymbol{\varepsilon}^0\right\} = \left[\boldsymbol{B}_p\right]\left\{\boldsymbol{u}_p\right\} \tag{12}$$

According to the derivation of Equation(11), $\frac{\partial \boldsymbol{K}_i}{\partial x_{ij}}$ can be expressed as:

$$\frac{\partial \boldsymbol{K}_i}{\partial x_{ij}} = \iint \begin{bmatrix} \boldsymbol{B}_p \\ \boldsymbol{B}_b \end{bmatrix}_i^{\mathrm{T}} \left(\sum_{n=1}^{m_L} \frac{\partial w_{in}}{\partial x_{ij}} \begin{bmatrix} \boldsymbol{A} & \boldsymbol{B} \\ \boldsymbol{B} & \boldsymbol{D} \end{bmatrix}_i^{(n)} \right) \begin{bmatrix} \boldsymbol{B}_p \\ \boldsymbol{B}_b \end{bmatrix}_i dxdy \tag{13}$$

Mathematically, the following relation can easily be derived:

$$\frac{\partial \boldsymbol{K}_i}{\partial x_{ij}} = \sum_{n=1}^{m_L} \frac{\partial w_{in}}{\partial x_{ij}} \iint \begin{bmatrix} \boldsymbol{B}_p \\ \boldsymbol{B}_b \end{bmatrix}_i^{\mathrm{T}} \begin{bmatrix} \boldsymbol{A} & \boldsymbol{B} \\ \boldsymbol{B} & \boldsymbol{D} \end{bmatrix}_i^{(n)} \begin{bmatrix} \boldsymbol{B}_p \\ \boldsymbol{B}_b \end{bmatrix}_i dxdy = \sum_{n=1}^{m_L} \frac{\partial w_{in}}{\partial x_{ij}} \boldsymbol{K}_i^{(n)} \tag{14}$$

To calculate the partial derivative of weight *w*, the interpolation scheme given in Equation (2) is used to produce.

$$\frac{\partial w_{in}}{\partial x_{ij}} = \begin{cases} p x_{in}^{p-1} \prod_{\substack{\xi=1 \\ \xi \neq n}}^{m} (1 - x_{i\xi}^{p}) & \text{if } j = n \\ -p x_{ij}^{p-1} x_{in}^{p} \prod_{\substack{\xi=1 \\ \xi \neq n \\ \xi \neq j}}^{m} (1 - x_{i\xi}^{p}) & \text{if } j \neq n \end{cases} \tag{15}$$

To begin the optimization process, the alternative angle combinations and stacking sequences for DD laminates must be selected according to the specific technological requirements. Next, the stiffness matrix is calculated for each angle combination, and the interpolated stiffness matrix is obtained through the UMLI scheme. Subsequently, the sensitivity is computed, the design variables are updated, and the response value is calculated by finite element analysis (FEA). The angle design of DD laminates is finalized once the convergence criterion is reached. In this work, the optimization is considered to have converged when the weights of each angle combination converge to 0 or 1. The calculations are stopped once the convergence condition is achieved. The specific flowchart is shown in Figure 4.

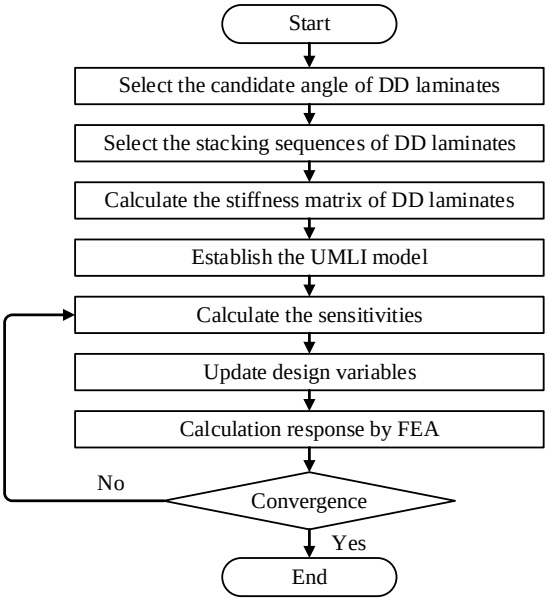

Figure 4 Optimization process flow chart

3 Results

Composite stiffened panels are frequently employed in the manufacture of wings and fuselages. The cross-section of the stiffener commonly assumes an "L" shape, "T" shape, "Ω" shape, and so on. In this example, the composite stiffened plate comprises one 40-ply curved plate and eight 40-ply L-shaped stiffeners of varying lengths, as illustrated in Figure 5. The common forming processes for composite stiffened panels can be used to connect different areas: co-curing, co-bonding, or secondary bonding. The stiffened panels are subjected to a pressure of 5000Pa and a shear force of 3000N.

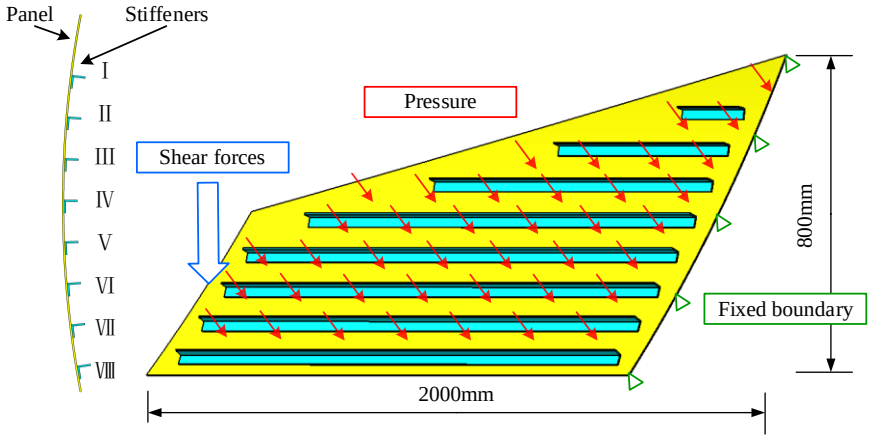

Figure 5 Composite stiffened panel with 8 L-shaped stiffeners.

In order to compare the effects of SD laminates and laminates with the same angle on the optimization results and compliance, an angle increment of 7.5 degrees was selected. There are 91 angle combinations, as shown in Figure 3. The horizontal axis represents the value of Φ, while the vertical axis represents the value of Ψ. The squares indicate the angle combination numbers. The red squares represent laminates with the

same angle, the blue squares represent SD laminates, and the green squares represent DD laminates. We used 91, 89 (excluding laminates with the same angle), and 78 (excluding SD laminates) as alternative angle combinations, with the goal of optimizing for minimum compliance. For the three examples, the initial value is set to 0.4 and the step size is 0.2. The angle combination selection for the obtained panel and stiffeners is presented in the following Table 1. The convergence curve is illustrated in Figure 6.

91 Angle combination	89 Angle combination	78 Angle combination
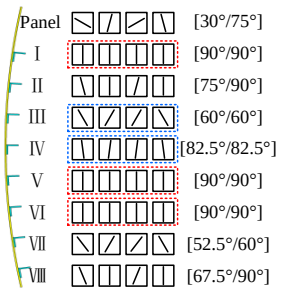	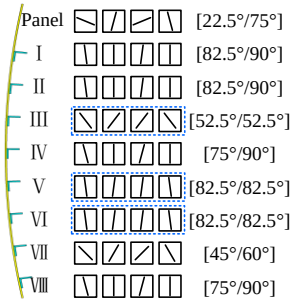	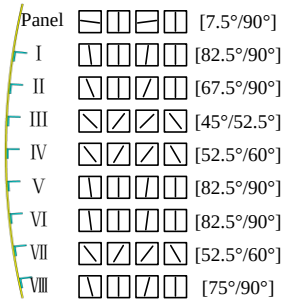
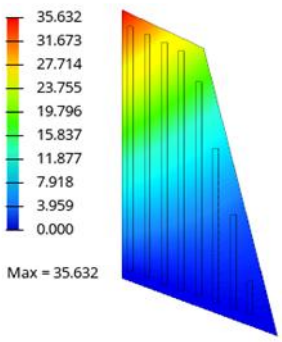	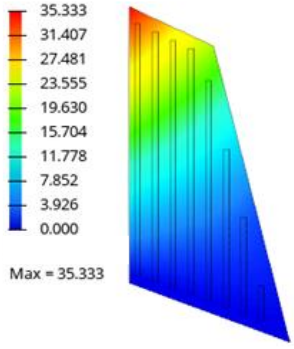	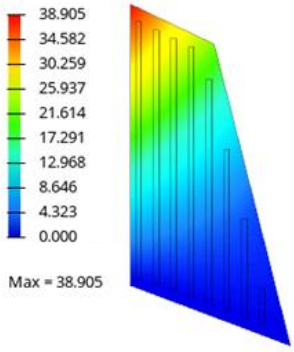

Table 1 Optimization results and finite element analysis results of composite stiffened panels.

The compliance converges to 2260J from 91 alternative angle combinations. The compliance converges to 2290J from 89 alternative angle combinations. The compliance converges to 2630J from 78 alternative angle combinations. The results of 91 alternative Angle combinations and 89 alternative Angle combinations are better because the 78 Angle combinations exclude SD laminates and cause a loss of mechanical properties. The difference between the results including SD and those excluding SD is about 14.8% in this example. Finite element analysis was conducted on the three optimized results, as shown in Table 1. It was found that the maximum displacements were 35.63mm, 35.33mm, and 38.91mm, which followed the same trend as the compliance results. When dealing with practical engineering problems, it is necessary to choose the appropriate alternative angle combinations according to the specific process requirements.

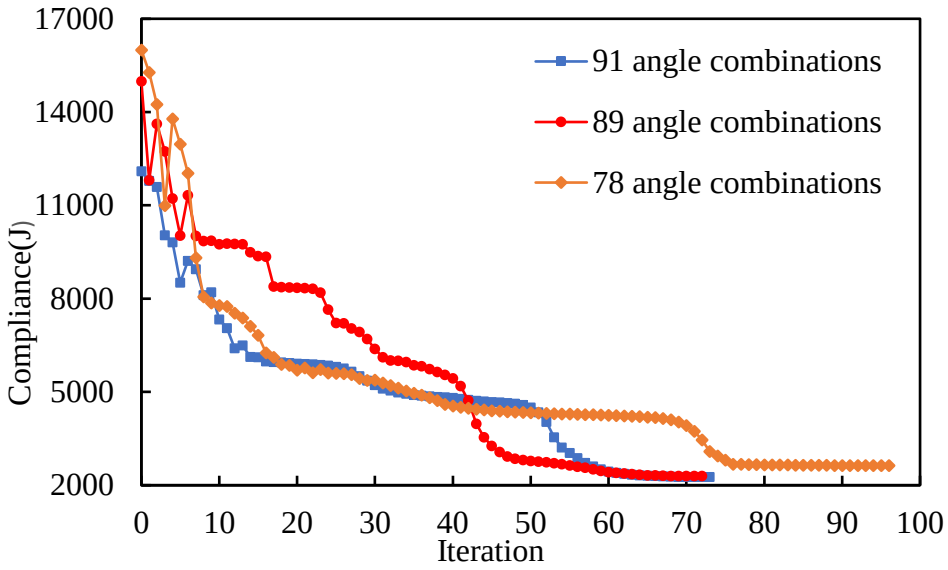

Figure 6 Convergence curve of compliance.

Due to its low cost, simple structure, and other advantages, the UAVs are widely used in military, meteorological, surveying, and other fields. The introduction of composite materials, which have high specific modulus and stiffness, can enable UAVs to have better performance, greater load capacity, and longer range. In this example, the UAV has a wingspan of 2m, and we calculate half of the wing. The wing is a two-spar wing, consisting of an upper skin, a lower skin, a front spar, a rear spar, and four wing ribs distributed along the span direction, as shown in Figure 7. All areas are made of 20 plies of 0.1 thick composite materials. The wing bears the upward lift acting on the skin surface, which is applied in the form of pressure, referred to as the lift condition in this paper; Due to the deflection of the wing control surface or gust load, the wing bears the torsional load, which is applied in the form of concentrated force, referred to as the concentrated force condition.

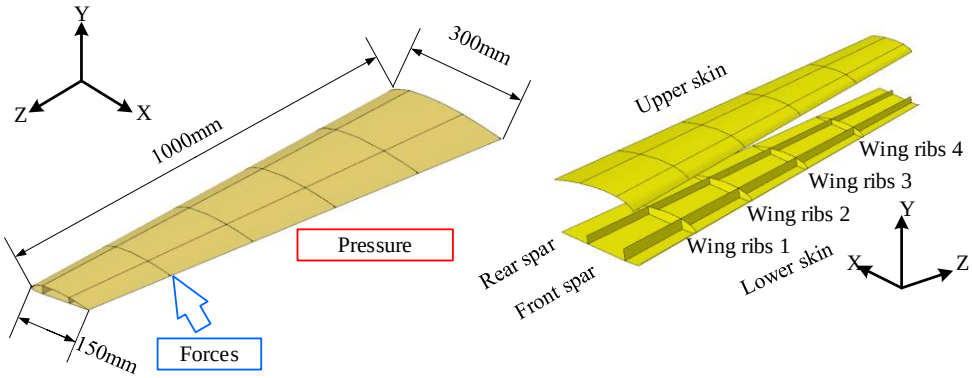

Figure 7 Composite UAV wings

In this example, an angle increment of 7.5 degrees was selected. The alternative angle combinations are shown in **Hiba! A hivatkozási forrás nem található.**. Considering the constraint of processability, the angle combinations [0/0] and [90/90] were removed. The remaining 89 alternative angle combinations were selected. The

optimization results considering lift condition and concentrated force condition were calculated. The initial value was set to 0.4 and the step size was set to 0.12. The convergence curve is shown in Figure 8. After 74 steps of calculation, the compliance converged to 268.8J stablely. To verify the correctness of the results, the lift condition, concentrated force condition, and coupled condition were verified for the DD-piled wing.

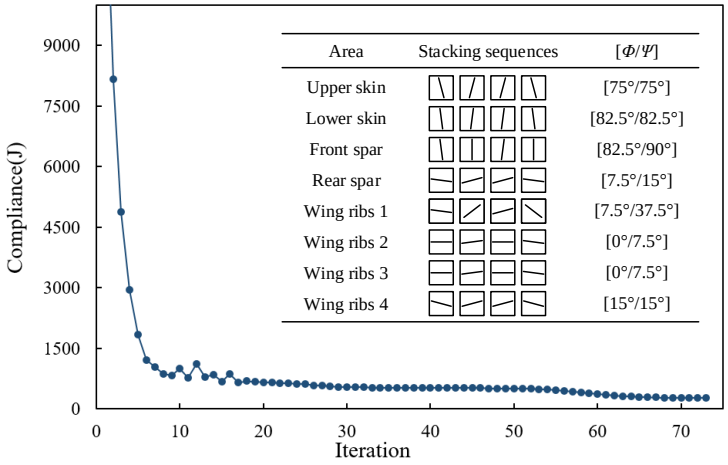

Figure 8 The convergence curve and the optimization results

For comparison, the Quad-piled wing was also calculated and the UMMI method is adopted to optimize the angle. The results of angle selection are shown in Table 2 Optimization results of Quad-piled wing with UMMI. Upon examination, it is evident that the UMMI optimization results exhibit numerous violations of design constraints, potentially posing significant challenges to manufacturability and giving rise to issues such as warping, delamination, and other defects in the formed composite parts.. The orange curve shows that the compliance converged to 454.8J, which is slightly greater than that of the DD-piled wing.

Area	layerups
Upper skin	$[90°_{11}/45°_{9}]$
Lower skin	$[90°_{2}/ -45°_{9}/ 0°_{2}/-45°_{6}/ 90°]$
Front spar	$[90°_{20}]$
Rear spar	$[0°_{20}]$
Wing rib 1	$[0°_{3}/45°_{8}/0°_{9}]$
Wing rib 2	$[90°/0°_{14}/-45°_{3}/ 90°]$
Wing rib 3	$[90°_{3}/0°_{9}/45°_{6}/90°_{2}]$
Wing rib 4	$[-45°_{10}/0°_{6}/-45°_{2}/90°_{2}]$

Table 2 Optimization results of Quad-piled wing with UMMI

In addition, in order to compare with the optimization results of commercial software, the stacking sequence of the Quad-piled wing was optimized using software-OPTISTRUCT. The initial four angles of the Quad-piled wing are equal in percentage, each accounting for 25%. The optimized stacking sequence is shown in Table 3. Simultaneously, the several commonly used Quad-piled wing is adopted for calculation: Commonly used Quad-piled wing – repeat, with the stacking sequence of

$[0,45,90,-45]_5$; Commonly used Quad-piled wing – symmetry, with the stacking sequence of $[0,45,90,-45,0,45,90,-45,0,45]_s$.

Area	layerups
Upper skin	$[-45°_5/45°_2/90°_2/45°_3/90°_3/\ 0°_5]$
Lower skin	$[90°/\ 0°_5/\ 45°_2/-45°/\ 90°/-45°_4/90°/45°_2/90°_2]$
Front spar	$[-45°/90°_5/\ 0°_3/45°_5/-45°_3/\ 0°_2/-45°]$
Rear spar	$[-45°/\ 0°_4/-45°/\ 0°/45°/90°/45°_4/-45°_2/90°_4/-45°]$
Wing rib 1	$[90°_2/\ 45°_5/0°_5/-45°_5/90°_3]$
Wing rib 2	$[90°_5/\ 45°/0°_5/-45°_4/45°/-45°/45°_3]$
Wing rib 3	$[90°_5/\ 45°/0°_5/-45°_5/45°_4]$
Wing rib 4	$[90°_2/\ -45°_3/45°/0°/-45°_2/0°_4/45°_4/90°_3]$

Table 3 Optimization results of Quad-piled wing with OPTISTRUCT

The results of the verification analysis of the DD-piled wing, the optimized Quad-piled wing and two commonly used Quad-piled wings are calculated. The histogram of maximum displacement comparison is shown in Figure 9.

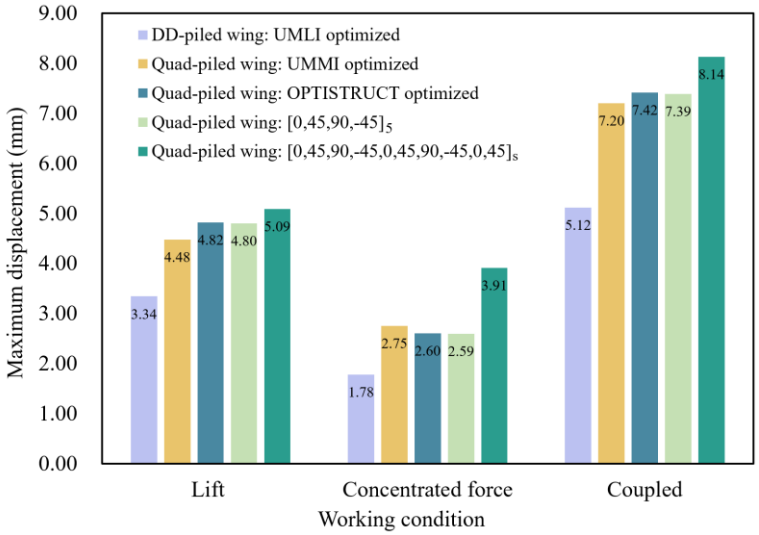

Figure 9 The maximum displacement comparison

As evident from the figure, In this example, The maximum displacement of Quad-piled wing optimized by UMMI, Quad-piled wing optimized by OPTISTRUCT, and Quad-piled wing with repeated layings is very similar, and the displacement of Quad-piled wing with symmetrical layings is slightly larger. In contrast, the DD-piled wing optimized by UMLI exhibits a reduction of approximately 30% in its maximum displacement, thereby validating the effectiveness of optimizing the DD-piled wing.

4 Conclusions and Contributions

This paper proposes an optimization design method for DD laminates based on multi-material topology optimization method. Based on the evolution of UMMI, an interpolation method UMLI for multi-layer structures is proposed. The optimization design of DD laminates is completed by interpolating the stiffness matrix of the laminates formed by each angle combination. The main conclusions are as follows:

(1) UMLI is suitable for the optimization design of multi-layer structures with certainty stacking sequence in the layer direction, such as DD laminates. And the optimization results show that the optimized DD laminates can achieve similar or better performance than QUAD laminates.
(2) The selection of alternative angles has a significant impact on the optimization results, and SD laminates and laminates with the same angle are better choices in some cases. In practical use, it is necessary to choose suitable alternative angles based on engineering process requirements.

This paper applies the method to the design of multi-area structures. In future work, this method can be applied to the angular design of variable stiffness DD laminates. At the same time, the performance and processability of DD laminates can be verified through experiments and simulation analysis.

Acknowledgements

This work is supported by the National Key Research and Development Program of China (2022YFB4602001)

References

[1] Y. Xu, J. Zhu, Z. Wu, Y. Cao, Y. Zhao, and W. Zhang, 'A review on the design of laminated composite structures: constant and variable stiffness design and topology optimization', Adv Compos Hybrid Mater, vol. 1, no. 3, pp. 460–477, Sep. 2018, doi: 10.1007/s42114-018-0032-7.

[2] A. Tiwary, R. Kumar, and J. S. Chohan, 'A review on characteristics of composite and advanced materials used for aerospace applications', Materials Today: Proceedings, vol. 51, pp. 865–870, 2022, doi: 10.1016/j.matpr.2021.06.276.

[3] T. Gao and W. Zhang, 'A mass constraint formulation for structural topology optimization with multiphase materials', International Journal for Numerical Methods in Engineering, vol. 88, no. 8, pp. 774–796, 2011, doi: 10.1002/nme.3197.

[4] E. Lund and J. Stegmann, 'On structural optimization of composite shell structures using a discrete constitutive parametrization', Wind Energ., vol. 8, no. 1, pp. 109–124, Jan. 2005, doi: 10.1002/we.132.

[5] Z. Duan, J. Yan, and G. Zhao, 'Integrated optimization of the material and structure of composites based on the Heaviside penalization of discrete material model', Struct Multidisc Optim, vol. 51, no. 3, pp. 721–732, Mar. 2015, doi: 10.1007/s00158-014-1168-x.

[6] N. L. Pedersen, 'On design of fiber-nets and orientation for eigenfrequency optimization of plates', Comput Mech, vol. 39, no. 1, pp. 1–13, Dec. 2006, doi: 10.1007/s00466-005-0002-0.

[7] B. Niu, Y. Shan, and E. Lund, 'Discrete material optimization of vibrating composite plate and attached piezoelectric fiber composite patch', Struct

Multidisc Optim, vol. 60, no. 5, pp. 1759–1782, Nov. 2019, doi: 10.1007/s00158-019-02359-8.
[8] M. C.-Y. Niu, Airframe structural design: practical design information and data on aircraft structures, 2. ed., 3. publ. with minor corr. Hong Kong: Conmilit Press Ltd, 2006.
[9] J. E. Herencia, P. M. Weaver, and M. I. Friswell, 'Optimization of Long Anisotropic Laminated Fiber Composite Panels with T-Shaped Stiffeners', AIAA Journal, vol. 45, no. 10, pp. 2497–2509, Oct. 2007, doi: 10.2514/1.26321.
[10] X. Liu, C. A. Featherston, and D. Kennedy, 'Two-level layup optimization of composite laminate using lamination parameters', Composite Structures, vol. 211, pp. 337–350, Mar. 2019, doi: 10.1016/j.compstruct.2018.12.054.
[11] N. Fedon, P. M. Weaver, A. Pirrera, and T. Macquart, 'A repair algorithm for composite laminates to satisfy lay-up design guidelines', Composite Structures, vol. 259, p. 113448, Mar. 2021, doi: 10.1016/j.compstruct.2020.113448.
[12] M. Bruyneel, C. Beghin, G. Craveur, S. Grihon, and M. Sosonkina, 'Stacking sequence optimization for constant stiffness laminates based on a continuous optimization approach', Struct Multidisc Optim, vol. 46, no. 6, pp. 783–794, Dec. 2012, doi: 10.1007/s00158-012-0806-4.
[13] S. W. Tsai, 'Double–Double: New Family of Composite Laminates', AIAA Journal, vol. 59, no. 11, pp. 4293–4305, Nov. 2021, doi: 10.2514/1.J060659.
[14] S. Shrivastava, N. Sharma, S. W. Tsai, and P. M. Mohite, 'D and DD-drop layup optimization of aircraft wing panels under multi-load case design environment', Composite Structures, vol. 248, p. 112518, Sep. 2020, doi: 10.1016/j.compstruct.2020.112518.
[15] K. Zhao, D. Kennedy, A. Miravete, S. W. Tsai, C. A. Featherston, and X. Liu, 'Defining the Design Space for Double–Double Laminates by Considering Homogenization Criterion', AIAA Journal, pp. 1–14, Mar. 2023, doi: 10.2514/1.J062639.
[16] B. Vermes, S. W. Tsai, T. Massard, G. S. Springer, and T. Czigany, 'Design of laminates by a novel "double–double" layup', Thin-Walled Structures, vol. 165, p. 107954, Aug. 2021, doi: 10.1016/j.tws.2021.107954.
[17] E. Kappel, 'Double–Double laminates for aerospace applications — Finding best laminates for given load sets', Composites Part C: Open Access, vol. 8, p. 100244, Jul. 2022, doi: 10.1016/j.jcomc.2022.100244.
[18] Y. Wang, D. Wang, Y. Zhong, D. W. Rosen, S. Li, and S. W. Tsai, 'Topology optimization of Double-Double (DD) composite laminates considering stress control', Computer Methods in Applied Mechanics and Engineering, vol. 414, p. 116191, Sep. 2023, doi: 10.1016/j.cma.2023.116191.
[19] S. W. Tsai, 'Expectation of the next generation research in composite materials', 2023.